A phosphoramidate substrate analog is a competitive inhibitor of the *Tetrahymena* group I ribozyme

Raven L Hanna [1], Sergei M Gryaznov [3] and Jennifer A Doudna [1,2]

Background: Phosphoramidate oligonucleotide analogs containing N3′–P5′ linkages share many structural properties with natural nucleic acids and can be recognized by some RNA-binding proteins. Therefore, if the N–P bond is resistant to nucleolytic cleavage, these analogs may be effective substrate analog inhibitors of certain enzymes that hydrolyze RNA. We have explored the ability of the *Tetrahymena* group I intron ribozyme to bind and cleave DNA and RNA phosphoramidate analogs.

Results: The *Tetrahymena* group I ribozyme efficiently binds to phosphoramidate oligonucleotides but is unable to cleave the N3′–P5′ bond. Although it adopts an A-form helical structure, the deoxyribo-phosphoramidate analog, like DNA, does not dock efficiently into the ribozyme catalytic core. In contrast, the ribo-phosphoramidate analog docks similarly to the native RNA substrate, and behaves as a competitive inhibitor of the group I intron 5′ splicing reaction.

Conclusions: Ribo-N3′–P5′ phosphoramidate oligonucleotides are useful tools for structural and functional studies of ribozymes as well as protein–RNA interactions.

[1]Department of Molecular Biophysics and Biochemistry, Yale University, New Haven, CT 06520-8114, USA
[2]Howard Hughes Medical Institute, Yale University, New Haven, CT 06520-8114, USA
[3]Geron Corporation, 230 Constitution Drive, Menlo Park, CA 94025, USA

Correspondence: Jennifer A Doudna
E-mail: jennifer.doudna@yale.edu

Introduction

Group I introns are catalytic RNAs capable of self-splicing from precursor transcripts. Hundreds of examples of group I introns, characterized by common secondary structural elements, have been identified in a variety of species [1,2]. The *Tetrahymena thermophila* intervening sequence of nuclear pre-rRNA, the first self-splicing intron discovered [3], has been characterized extensively and is used as a model system [4]. The secondary structure of the wild type *Tetrahymena* group I intron is shown in Figure 1a. The splicing reaction performed by the intron occurs through a two-step *trans*-esterification mechanism (Figure 1b). In the first step, the intron binds an exogenous guanosine nucleotide (G_e), positioning its 3′-hydroxyl for nucleophilic attack on the phosphate at the 5′ splice site. Following strand scission at the 5′ exon–intron junction, the 3′-hydroxyl group of the cleaved 5′ exon attacks the phosphate at the 3′ splice site to produce ligated exons and a free intron, which retains catalytic activity [5–7]. Several specifically positioned magnesium ions are essential for RNA structure stability and transition state stabilization [8–10]. Group I introns are often studied as multiple turnover enzymes by separating the 5′ exon from the intron and deleting the 3′ exon [11]. These engineered constructs (L-18-ScaI, L-21-ScaI) cleave a short oligonucleotide substrate using an exogenous guanosine (G_e), analogous to the first step of the native reaction (Figure 1c). The ribozyme can also be engineered to perform the reverse of the second step of the reaction. In these ribozyme constructs (L-18-ωG, L-21-ωG), the terminal G (G_ω) serves as the attacking nucleophile to cleave short oligonucleotide substrates in *trans* (Figure 1d), causing the intron to become covalently attached to the reaction product.

The *Tetrahymena* group I ribozyme binds a *trans*-substrate in two steps: duplex formation and docking. Duplex formation is accomplished through Watson–Crick base pairing of the substrate to the internal guide sequence (IGS). This duplex, termed P1, then docks into the reaction core through a number of tertiary interactions involving hydrogen bonds to 2′-hydroxyl groups of the substrate backbone [12]. Deoxyribose-containing substrates, which lack the 2′-hydroxyl groups, are unable to efficiently dock into the reaction core and hence are much less reactive than RNA substrates [13,14]. In addition to tertiary interactions between the substrate and the ribozyme core, binding of metal ions and the guanosine co-substrate contribute to substrate docking efficiency [15].

Available crystal structures of parts of the *Tetrahymena* group I intron [16,17] are not complete or detailed enough to put the reaction mechanism into a structural context.
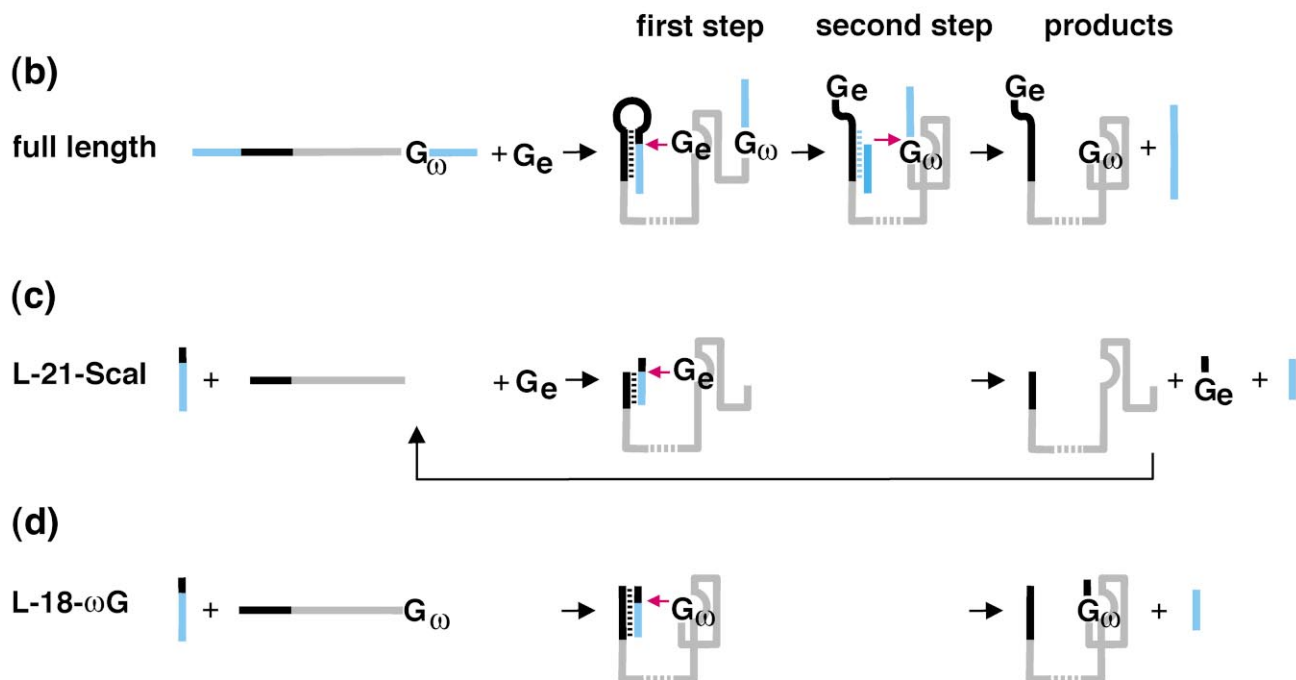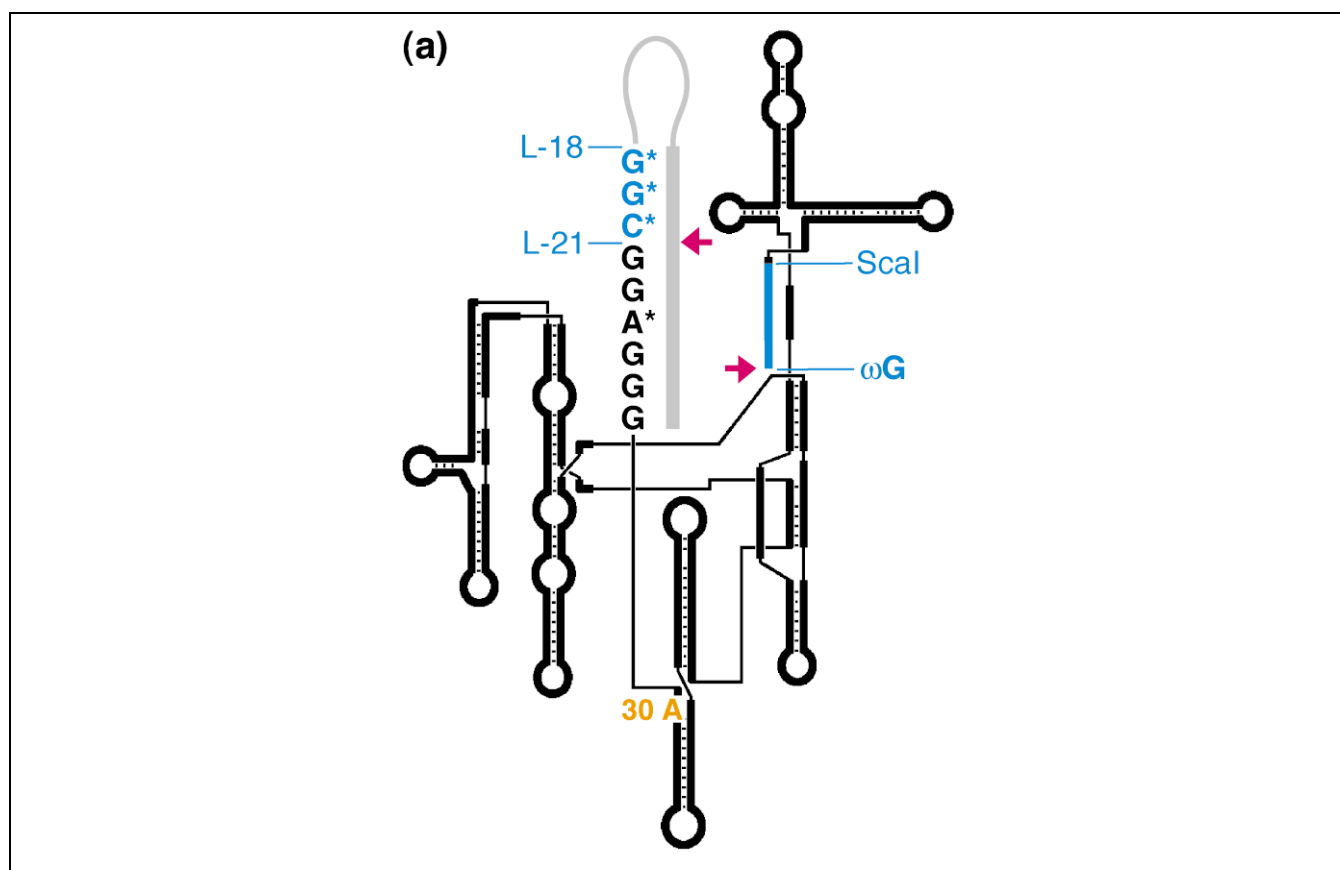
Figure 1. The *T. thermophila* group I intron. **(a)** Secondary structure diagram of the *Tetrahymena* group I intron. Magenta arrows mark the 3′ and 5′ splice sites. The four ribozyme constructs used in these experiments are combinations of the length variants marked in blue. The additional 5′ nucleotides present in the *cis*-acting wild type molecule are shown in gray. Sequences are identical between the variants, except the A denoted by an asterisk in the P1 stem, which is an A in the wild type intron and the L-18 constructs, but a U in the L-21 constructs. The cyan nucleotides marked by asterisks have been changed from uracils, to ensure efficient transcription with bacteriophage T7 RNA polymerase. A30, highlighted in orange, becomes accessible to DMS upon substrate docking. Schematic diagrams of **(b)** the *cis*-reaction of the natural group I intron, **(c)** the multi-turnover *trans*-reaction of an engineered construct (L-21-ScaI), and **(d)** the single turnover *trans*-reaction of an engineered construct (L-18-ωG) are shown. The flanking exons are colored dark blue. Mapped on to the gray body of the group I intron is the P1 substrate helix in black. G_e is the exogenous guanosine co-factor and $G_ω$ is the terminal guanosine of the intron. Magenta arrows are drawn between the nucleophile and labile bond for each step of the reactions.
←

Structural studies to elucidate the mechanism have been difficult because no known substrate analog could completely inhibit the cleavage reaction while leaving the reaction core structurally intact. DNA oligonucleotides or RNA oligonucleotide analogs containing 2′-deoxy or phosphorothioate substitutions decrease the reaction rate [13,18], but this is more likely due to improper substrate docking rather than direct inhibition of the chemical step. Detailed structural analysis of the group I ribozyme reaction mechanism will be aided by non-cleavable substrate analogs that more closely mimic the properties of the RNA substrate.

The increasing interest in using nucleic acid analogs for clinical purposes has led to development of chemically stable analogs of DNA and RNA. The N3′–P5′ phosphoramidate nucleic acid analogs, where each 3′-oxygen is replaced by a 3′-amino group (Figure 2), are promising antisense agents [19–22] as well as potential tools for basic research in the field of RNA structure and chemistry. Although protonation of the nitrogen in acidic conditions causes degradation, these analogs are stable at physiological pH [23]. Phosphoramidate DNA oligonucleotides [24]

form RNA-like A-form duplexes which are more thermally stable than RNA or DNA helices of the same sequence [25,26]. They also form specific and stable heteroduplexes with natural nucleic acids, including triple helices [27], and they show significant nuclease resistance [28]. Furthermore, helices composed of the phosphoramidate DNA analog can function as RNA mimics which can be specifically recognized by RNA-binding proteins, such as HIV Rev and Tat, presumably due to their preference for RNA-like helical geometry [29,30]. The phosphoramidate DNA analog has also been used to prevent substrate binding to the *Pneumocystis carinii* group I intron [31,32]. More recently, the synthesis of phosphoramidates containing 2′-hydroxyl groups was reported [23,33]. These analogs can also form heteroduplexes and triplexes with RNA and DNA which are significantly more stable than their phosphodiester counterparts.

Based on their structural and chemical properties, the phosphoramidate-containing oligonucleotide analogs are good candidates for substrate analog inhibitors to the group I intron ribozyme. We show here that a phosphoramidate RNA analog is a competitive inhibitor of the *Tetrahymena*
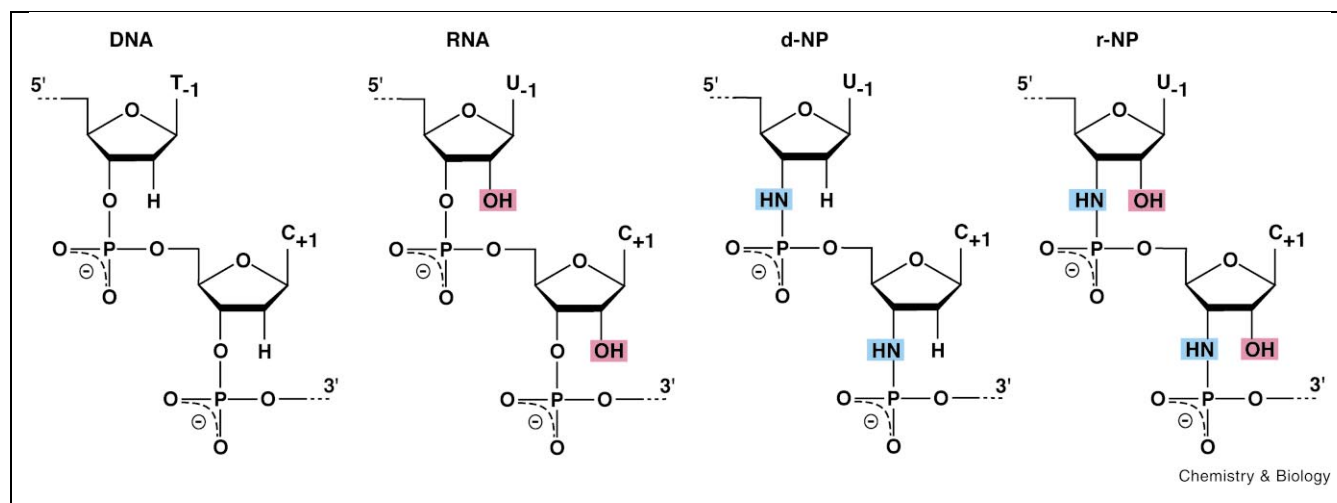

Figure 2. The chemical structures of the substrates and analogs. The sugars of two representative nucleotides from the four 9-mer oligonucleotides used in this study have been drawn, and the chemical differences are highlighted.
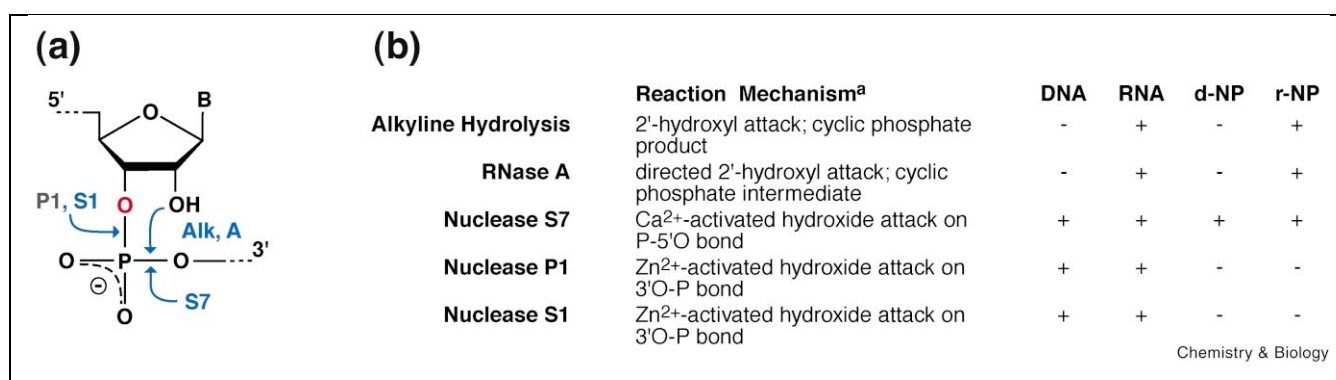
Figure 3. Nuclease cleavage of phosphoramidate analogs. **(a)** Cleavage sites of the nucleases used are marked in blue. The 2′-oxygen, highlighted in red, is exchanged for a nitrogen in the phosphoramidate analogs. **(b)** The ability for each oligonucleotide to be cleaved by the various chemical and enzymatic mechanisms is denoted with a plus or minus. [a]See [48,49].

group I intron ribozyme. This substrate mimic binds to the ribozyme active site like the native substrate but is completely unreactive. Unlike other group I intron substrate analogs, the phosphoramidate oligonucleotide blocks RNA-catalyzed transesterification chemically rather than by perturbing active site structure.

Results and discussion

Four 9 nucleotide (9-mer) substrates (Figure 2) isosequential to the 5′ half of the P1 substrate helix (5′-CUCU-CUGCC) were used to compare the properties of the 2′-deoxy phosphoramidate (d-NP) and the 2′-hydroxyl phosphoramidate (r-NP) analogs to DNA and RNA substrates. To determine whether the N–P bond confers increased stability against enzymatic activity, the various substrates were subjected to alkaline hydrolysis and enzymatic cleavage agents (Figure 3). Like RNA, the r-NP analog is sensitive to alkaline hydrolysis, demonstrating that, despite the nitrogen substitution, the 2′-hydroxyl is able to attack the adjacent phosphate and cleave the P–O5′ bond, creating a cyclic phosphate product. Similarly, RNase A, which cleaves RNA via a cyclic phosphate intermediate, recognizes and cleaves the r-NP backbone. Micrococcal nuclease (S7) catalyzes hydrolysis of the P–O5′ bond of DNA and RNA through a nucleophilic in-line attack [34] and is able to cleave both d-NP and r-NP. However, nucleases P1 and S1, which both target the O3′–P bond, are not able to cleave the N–P oligonucleotides. Despite the difference in bond specificity, the active site of nuclease P1 has a similar arrangement to nuclease S7 [35]. This suggests that specific properties of the N–P bond render it resistant to nucleolytic cleavage by the nucleases P1 and S1 yet still allow adjacent bonds to maintain their usual chemical functionalities, such as susceptibility to nuclease S7 cleavage. The L-18-ScaI *Tetrahymena* ribozyme, which catalyzes the nucleolytic cleavage of the O3′–P bond, was tested for its ability to cleave the d-NP and r-NP analog molecules using

standard reaction conditions (Figure 4). No cleavage of either of the N–P analog oligonucleotides occurred after even 10 days of incubation, which corresponds to at least a 10 000-fold decrease in reaction rate for both of the analogs.

The lack of N–P analog cleavage by the catalytic RNA could be due to a disruption of any part of the substrate binding and cleavage pathway for the ribozyme. Base pairing to the IGS, docking of the resulting duplex into the ribozyme active site, and/or the chemical step of the reaction could be disrupted by the presence of the N–P bond. Apparent dissociation constant ($K_{\mathrm{d}}^{\mathrm{app}}$) values of the ribozyme–substrate complexes were measured to determine whether the phosphoramidate bond disrupts complex formation (Table 1). For the *Tetrahymena* group I ribozyme, the product RNA binds more tightly to the ribozyme than the substrate RNA [36]. For comparison, the apparent K_{d} of the 6-mer product RNA and the L-18-ScaI ribozyme

Table 1

Stability of the substrates bound to the ribozymes: K_{d} (nM) values.

	L-18-ωG	L-18-ScaI	L-21-ωG	L-21-ScaI
R6	n.d.[a]	0.1 ± 0.05	n.d.	2 ± 0.5
DNA	>1000	>1000	>1000	>1000
RNA	n.d.	2.7 ± 0.2	n.d.	2.9 ± 0.8
d-NP	11 ± 1	16 ± 3	45 ± 5	90 ± 10
r-NP	2.6 ± 0.2	6.5 ± 0.5	4.6 ± 0.4	1.4 ± 0.3

Equilibrium dissociation binding constants measured from gel shift experiments. $K_{\mathrm{d}}^{\mathrm{app}}$ values are in nM. This assay was not sensitive above 1000 or below 0.1 nM.
[a]Binding constants for the RNA 9-mer substrate and the RNA 6-mer product with the ribozymes containing the 3′ terminal G were not determined (n.d.) due to cleavage. Binding constants between RNA substrate and the ribozymes truncated at the ScaI site are not at equilibrium, since the oligonucleotide is susceptible to ribozyme-directed hydrolysis.
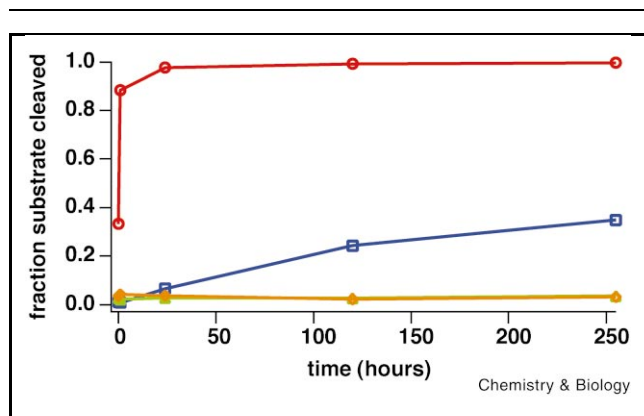
Figure 4. Fraction substrate cleaved vs. time. The four substrates (DNA, blue squares; RNA, red circles; d-NP, green triangles; r-NP, orange diamonds) were incubated with L-18-ScaI ribozyme. Percent substrate cleaved was plotted for five time points: 1.5 min, 1 h, 1 day, 5 days, and 10 days. Parallel reactions without ribozyme showed no cleavage, except for minor background hydrolysis of the RNA substrate (less than 5% cleaved in 10 days).

was found to be 0.1 nM (−13.6 kcal/mol), which is similar to values measured previously under similar conditions [12,37,38]. The low affinity of DNA substrates for the ribozyme has been shown to result from poor docking due to the lack of tertiary interactions mediated by substrate 2′-hydroxyl groups and the adoption of a different helical conformation [18]. The d-NP analog binds the ribozyme quite efficiently, despite the inability to form tertiary interactions, which is likely due to the increased propensity to form an RNA-like helical structure. The values for r-NP oligonucleotide binding are similar to those for the RNA substrate, suggesting that there is no significant disruption of duplex formation. As with the d-NP analog, the decrease in P1 helix length between the L-18 and L-21 constructs (Figure 1d) causes a 0.8 kcal/mol destabilization in the r-NP analog bound to the ribozymes ending at the ScaI site. The values for r-NP analogs bound to ribozymes containing the terminal guanosine residue, which has a cooperative affect on substrate docking when bound in the G-binding site, show the opposite trend, having a small increase in complex stability for the shorter P1 helix when G_ω is present. Therefore, these observed K_d^{app} values reflect the opposing forces of substrate binding: helix stabilization is maximized by a longer helix, while substrate docking is more efficient with a shorter helix.

While N–P oligonucleotides are capable of efficient binding to the *Tetrahymena* ribozyme, the observed lack of cleavage might be caused by improper docking rather than inhibition of the chemical step. To test this possibility, dimethyl sulfate (DMS), which methylates the N1 of A residues, was used to test substrate docking into the ribozyme core. The adenosine at position 30 (A30, Figure 1d),

which resides at the base of P1 in the intron, is readily modified by DMS when the ribozyme is bound to a docked RNA substrate or cleavage product, but remains unmodified when bound to an oligo incapable of forming tertiary interactions [39]. Samples of L-18-ωG RNA (Figure 1c,d) complexed with DNA, RNA, or N–P analog oligonucleotides were treated with DMS and the sites of DMS modification were identified by reverse transcription (Figure 5a). There is no modification of A30 in the absence of magnesium, a condition under which the ribozyme is unfolded, or in a folded ribozyme without substrate. Ribozymes bound to the DNA substrate, which is unable to efficiently dock into the active site, show a low degree of modification at A30, while the ribozymes bound to the RNA substrate have strong methylation at A30. The complex with the d-NP oligonucleotide, as with DNA, shows little modification and therefore is apparently undocked, while the strong modification of A30 in the r-NP complex suggests efficient docking, similar to the RNA substrate.

To further evaluate the structural properties of the ribozyme–substrate complexes, labeled substrates pre-bound to the L-18-ScaI ribozyme were subjected to native poly-
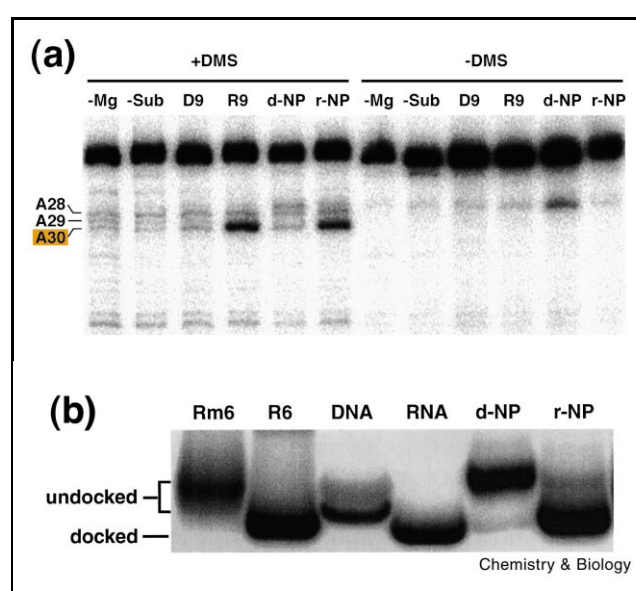

Figure 5. Docking of the substrates into the ribozyme core. **(a)** DMS chemical modification of L-18-ScaI ribozyme with the substrates. Ribozyme molecules modified with DMS while complexed to various substrates were reverse-transcribed using a 5′ end-labeled DNA primer. A30 is protected when the substrate is not docked and is deprotected when the substrate is docked. **(b)** Non-denaturing (native) gel of 5′ end-labeled substrate complexed to the L-18-ScaI ribozyme. The RNA cleavage 6-mer oligonucleotide (R6) and the RNA substrate serve as markers for properly docked complexes, while an RNA 6-mer oligonucleotide with a single 2′-O-methyl substitution (Rm6) and the DNA are undocked.
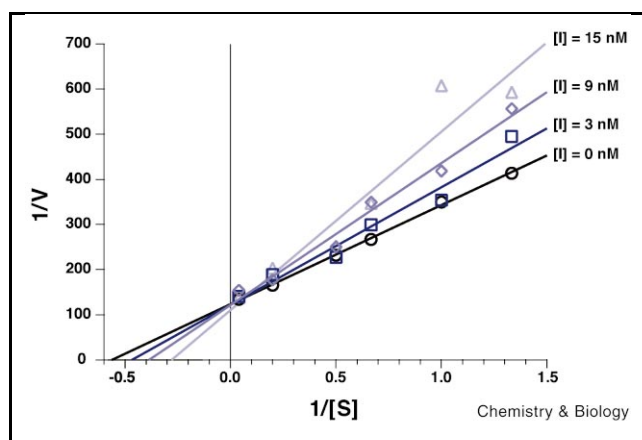
Figure 6. Reaction inhibition by the N–P RNA analog. Lineweaver–Burk plot of 1/[S] vs. 1/V at various inhibitor concentrations ([I]).

acrylamide gel electrophoresis, in which the overall shape, size, and charge of molecules in their folded state determine the rate of migration (Figure 5b). The docked RNA substrate/ribozyme and product/ribozyme complexes have a slightly increased mobility compared to the undocked complexes, such as those bound to DNA or an RNA 6-mer oligonucleotide containing a 2'-O-methyl modification at the −3 position [40]. A gel shift using the L-21-ScaI ribozyme, which has a shorter P1 duplex, is less pronounced (data not shown), supporting the theory that the lower migration rate of undocked complexes is caused by exposure of the P1 helix. Ribozymes bound to r-NP migrate at the same rate as the docked complexes, RNA 9-mer and 6-mer. Those bound to d-NP migrate more slowly, as do those complexed to DNA and −3-O-methylated RNA oligonucleotides, which do not dock efficiently [12,40]. These data suggest that the r-NP analog docks properly into the reaction core, while the d-NP analog does not.

The similarity in behavior of ribozymes complexed with r-NP oligonucleotides to those complexed with the RNA substrate indicates that the substrate analog probably inhibits the chemical step of the reaction and is a competitive inhibitor of the ribozyme reaction with native RNA substrate. A competitive inhibitor slows an enzymatic reaction by reversibly binding to the substrate binding site, thereby excluding the substrate. The hallmarks of competitive inhibition are a constant maximum velocity (V_{max}) and an increase in the apparent Michaelis constant (K_M^{app}) when the inhibitor is present [41]. To test whether the r-NP substrate analog exhibits these properties, the L-21-ScaI (Figure 1b,d) ribozyme was used under multiple turnover conditions, containing excess RNA substrate and guanosine co-factor. Using these experimental conditions, the

value of k_{cat} (turnover number) is 0.08 min^{-1} and k_{cat}/K_M (specificity constant) is 4.5×10^7 M^{-1} min^{-1}, which are similar to previously measured values [11,37]. The initial velocity of this reaction was measured at four inhibitor concentrations (0, 3, 9, and 15 nM), with each of six substrate concentrations (0.75, 1, 1.5, 2, 5, and 25 nM). A Lineweaver–Burk plot of these data (Figure 6) shows that V_{max} remains unaltered upon the addition of inhibitor, while the slope, K_M^{app}/V_{max}, increases as the inhibitor concentration increases, demonstrating competitive inhibition.

The r-NP substrate analog acts as a competitive inhibitor by binding specifically and tightly to the ribozyme and docking into the reaction core. Why does it resist cleavage by the ribozyme? Previous work has shown that an essential divalent metal ion directly coordinates the 3'-oxygen of the substrate at the cleavage site (Figure 7). Nitrogen, which replaces this oxygen in the analogs, does not coordinate magnesium as readily [42]. If inefficient metal ion coordination is responsible for the lack of ribozyme-mediated cleavage of the N–P linkage, adding 'soft' metal ions, which are able to coordinate nitrogen more efficiently, may rescue the activity. Three 'soft' metal ions, manganese, zinc and cadmium, were individually added to the cleavage
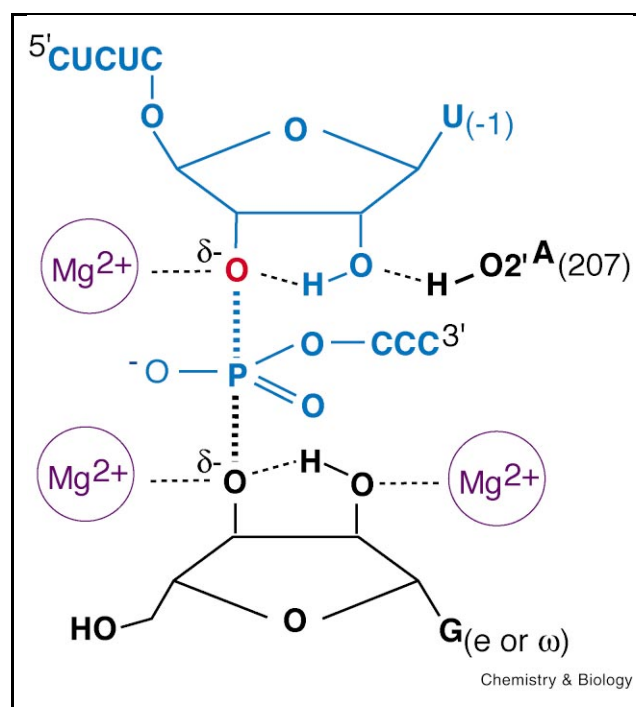

Figure 7. *Tetrahymena* group I intron transition state diagram. The substrate strand is shown in blue and the 2'-oxygen, which is exchanged for a nitrogen in the phosphoramidate analogs, is red. Three magnesium ions and a nucleotide triad help to stabilize the transition state [8–10,50].

assay, and the reactions were followed for 10 days (Figure 8). Neither manganese nor cadmium affect the rate of the reaction, but there is a slight decrease in the rate of RNA cleavage and an increase in the rate of DNA cleavage in the presence of zinc. This may be due to a zinc-induced distortion of the geometry of the active site, which could lower the energy barrier of the substrate helix docking for DNA, but may disrupt RNA-binding. The d-NP and r-NP analogs do not show cleavage in the presence of any of the 'soft' metal ions. These observations suggest that inefficient magnesium ion coordination is not the key inhibitory factor, but do not rule out this possibility completely. Another possibility is that slight geometric differences between RNA and r-NP in the docked core could account for the lack of reactivity. This seems unlikely since the core is flexible enough that even DNA, which is unable to form critical tertiary interactions, is slowly hydrolyzed. It is more likely that the ribozyme is chemically unable to hydrolyze the N3′–P5′ bond.

The group I intron has been shown to utilize a bimolecular nucleophilic substitution (S_N2) reaction mechanism [6,43]. The rate of an S_N2 reaction depends upon the solvation of the components, the steric accessibility of the electrophile, the nucleophilicity of the attacking group, and the nucleofugality of the leaving group. In the *Tetrahymena* ribozyme system, the effect of solvation can be excluded since the reaction takes place within a solvent inaccessible active site. The hydrogen on the 3′-amino group is the only steric addition and is not likely to affect the positioning of the phosphate oxygens in a manner that would exclude the attack of the nucleophile. The nucleophilicity of the attacking oxygen becomes important when considering the electrophilicity of the leaving group. In the pentavalent transition state structure (Figure 7), charge from the nucleophile is transferred to the leaving group, so that each has a partial negative charge [44]. The better the leaving group, compared with the nucleophile, the faster the reaction will progress. Both hydroxyls and amines are considered to be poor leaving groups because their basicity precludes the ability to readily support the extra negative charge. To improve the 3′-oxygen as a leaving group, the ribozyme positions cations which directly, and through a hydrogen bonding network, help support distribution of the negative charge. It is possible that this network is disrupted when oxygen is substituted by nitrogen, either due to disrupted metal ion coordination as discussed above or as a consequence of having an extra proton in the catalytic site. Even if the hydrogen bonding network is able to form, negative charge may not transfer to the amino leaving group in the transition state, because it is a poorer leaving group relative to the hydroxyl nucleophile. Additionally, the proposed interaction between the lone electron pair on the nitrogen and the σ* antibonding orbital of the phosphate [30] would increase the energy of the N–P bond, perhaps rendering it an even poorer leaving group.
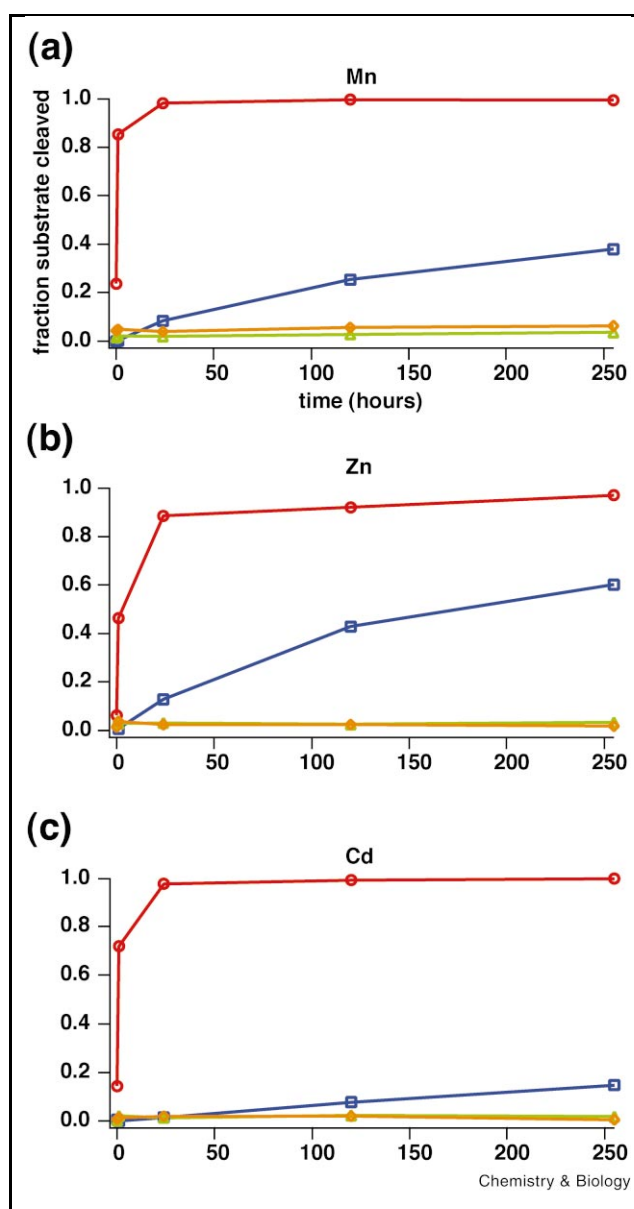

Figure 8. Plots of fraction substrate cleaved vs. time in the presence of soft metal ions. The four substrates (DNA, blue squares; RNA, red circles; d-NP, green triangles; r-NP, orange diamonds) were incubated with L-18-ScaI ribozyme with 2 mM **(a)** magnesium chloride, **(b)** zinc chloride, or **(c)** cadmium chloride. Fraction substrate cleaved was plotted for the five time points taken: 1.5 min, 1 h, 1 day, 5 days, and 10 days. Parallel reactions without ribozyme showed no cleavage.

Although the reduced nucleofugality of the amine leaving group is likely to cause a decrease in reaction rate, it may not fully explain the observed $> 10\,000$-fold decrease. An increased stability of the electrophile may discourage nucleophilic attack. A pseudo five-membered ring caused by the formation of a hydrogen bond between the amine and the 2′-oxygen, sharing either hydrogen, would facilitate the

formation of a double bond between the nitrogen and phosphate. Such an arrangement would cause the phosphorous atom to be less electrophilic, and, therefore, less susceptible to nucleophilic attack. The steric and electronic flexibility of the nitrogen could allow the double bond to occur, whereas an oxygen atom would prefer to remain in an sp^3 orbital state.

The inhibitory properties of the phosphoramidate oligonucleotide analogs are not limited to the *Tetrahymena* ribozyme system. The 200 nucleotide *Azoarcus* sp. *bh72* group I intron is also able to bind the d-NP analog without catalyzing cleavage (data not shown). Therefore, the phosphoramidate analogs may be useful as general inhibitors for all group I introns. Furthermore, these properties may also hold for other RNA or protein enzymes which act on RNA substrates through nucleophilic attack and cleavage of the O3′–P5′ bond.

Significance

The N3′–P5′ phosphoramidate RNA analog is the first group I ribozyme inhibitor identified to mimic native RNA substrate binding interactions, while being completely inert to cleavage. This substrate analog inhibitor binds tightly to RNA, forming helices more thermally stable than those of analogous RNA–RNA duplexes, and can form tertiary interactions with RNA. Some protein-based enzymes recognize the analog as RNA and cleave the P–5′O bond. Yet, neither the nucleases tested nor the *Tetrahymena* ribozyme were able to cleave the 3′N–P bond. Displaying many properties of RNA, this inhibitor may prove to be a useful tool for studying the structure and chemistry of enzymes that act on RNA.

The cleavage properties of the r-NP analog lead to the prediction that the small ribozymes which use a cyclic phosphate intermediate, such as HDV, VS, and hammerhead, would be able to cleave phosphoramidate oligonucleotides. However, it is likely that r-NP linkage would be an effective inhibitor for the group II intron, the spliceosome, and RNase P, which use a similar mechanism to the group I intron.

Furthermore, the recognition of this nucleic acid analog by proteins and RNA enzymes, in addition to the analog's increased stability in vivo, may have consequences for its adaptation for other uses, such as in vitro diagnostics or gene therapy.

Materials and methods

Preparation of ribozyme RNA
Genes encoding the RNA constructs utilized in this study were amplified from a plasmid containing the wild type *T. thermophila* group I intron sequence using PCR and cloned into pUC19 vectors behind the bacteriophage T7 RNA polymerase promoter sequence [45]. Plasmids were linearized for run-off transcription with either *Sca*I or *Bam*HI restriction endonuclease. RNAs were transcribed in vitro using T7 RNA polymer-

ase in transcription buffer (25 mM Tris–Cl, pH 8.0, 25 mM MgCl₂, 4 mM dithiothreitol, 0.01% (w/v) Triton X-100, 2 mM spermidine, 4 mM each NTP, 0.06 µg/µl linearized plasmid, 2 µg inorganic pyrophosphatase) and incubated at 37°C for 3–4 h. The transcripts from the plasmids digested with *Bam*HI carry out site-specific self-hydrolysis at the 3′ splice site during the incubation. The transcripts were subsequently purified on a stacked semi-denaturing gel (4 and 7% polyacrylamide, 1×TBE, 1 M urea). The bands were visualized by UV shadowing, excised, diced, frozen at −80°C for 10 min, and allowed to elute in water overnight at room temperature. The elutions were then filtered through a 0.2 micron filter, concentrated and de-salted, and stored at room temperature in water. Preceding each experiment, 14 nM ribozyme was annealed by heating in annealing buffer (50 mM Tris–Cl, pH 7.5, 10 mM MgCl₂, 10 mM NaCl, 0.1 M EDTA) at 50°C for 10–15 min, then allowed to slow cool to 25°C.

Preparation of substrates
The synthetic DNA 9-mer substrate (Keck Synthesis Lab, Yale University) was extracted with 10 volumes of *n*-butanol, precipitated with 2.5 volumes of ethanol and stored in water at −20°C. The RNA 9-mer substrate and 6-mer product (Dharmacon Research Inc.) were deprotected as described [46] and subsequently purified by high performance liquid chromatography using MonoQ HR and C18 reverse phase columns. The N–P analogs were synthesized and purified as described previously [33]. Substrates were 5′ end-labeled with ³²P using T4 polynucleotide kinase, purified through denaturing gel electrophoresis on a 20% polyacrylamide gel, and ethanol-precipitated.

Ribozyme cleavage assay
Annealed L-18-ScaI ribozyme was incubated at a concentration of 50 nM in annealing buffer, 2 mM GTP, and 0.01 mg/ml tRNA at 25°C. Trace amounts of 5′ end-labeled substrate were added to a final concentration of 1 nM to initiate reactions and overlaid with mineral oil to prevent sample concentration due to water evaporation during the long incubations. Aliquots at each time point were removed and quenched with two volumes of 10×FLB+EDTA (0.5×TBE, 80% formamide, 80 mM EDTA, 0.1% bromophenol blue, 0.05% xylene cyanol) and stored at −20°C. Reaction products were separated by electrophoresis on a 20% polyacrylamide, 1×TBE, 7 M urea gel and the fraction cleaved was quantified using a PhosphorImager and ImageQuant software (Molecular Dynamics (MD)). Reactions with soft metals were performed identically, with the addition of 2 mM MnCl₂, ZnCl₂, or CdCl₂ to the reaction buffer.

K_d binding constants
Apparent dissociation constants were measured using a native polyacrylamide gel electrophoresis mobility shift assay. Ribozyme was annealed as stated above and diluted in annealing buffer with 0.01 mg/ml tRNA. Concentrations of ribozyme ranging from 0.001 to 10 000 nM were incubated with a trace amount (>0.01 pM) of 5′ end-labeled oligonucleotide in a buffer containing annealing buffer, 0.01 mg/ml tRNA, 4% glycerol, and 0.05% xylene cyanol. Reactions were incubated at 25°C for 22–26 h, followed by separation of bound and unbound oligonucleotides by electrophoresis through an 8% polyacrylamide gel containing 10 mM Tris–HEPES, pH 7.5, 0.1 mM EDTA (1×THE) and 10 mM MgCl₂, at 25°C. The ratio of bound to unbound substrates was quantified using a PhosphorImager (MD) and fit to the equation: $\theta = (([E]_0 * a)/([E]_0 + K_d)) + b$, where θ is fraction bound, $[E]_0$ is the initial concentration of enzyme, and K_d is the apparent dissociation constant. The K_d values from at least three trials were averaged for each oligonucleotide–ribozyme combination.

DMS chemical probing
Reactions containing 20 nM of L-18-ωG ribozyme were annealed at 50°C for 20 min in annealing buffer then slow cooled to 42°C. Substrates 5′ end-labeled with ³²P were added at concentrations 5–10–

fold above the K_d. Reactions were allowed to equilibrate for 20 min prior to addition of DMS to a final concentration of 0.4%. After 7 min, the reactions were quenched by adding 200 mM β-mercaptoethanol and 15 μg tRNA. Reactions were precipitated twice with ethanol, then immediately reverse-transcribed using a primer extension protocol previously described [47].

Native polyacrylamide electrophoresis

10 μM L-18-ωG ribozyme was annealed with 5′ end-labeled oligonucleotides (1 μM RNA 9-mer, d-NP 9-mer, r-NP 9-mer, RNA 6-mer, or −3 methyl RNA 6-mer or 10 μM DNA 9-mer) in annealing buffer (see above) and 10% glycerol at 50°C for 15 min. Reactions were cooled to 30°C over 4 h then run on a 8% polyacrylamide, 5 mM MgCl$_2$, 1×THE, pH 7.5 native gel with the dimensions 15×24×0.1 cm at a constant wattage of 10 W for 12 h.

Kinetic experiments

Multiple turnover experiments were preformed using 1 nM L-21-ScaI ribozyme with 2 mM GTP ($K_d^G \sim 200$ μM [15]) in 1×annealing buffer (see above) with 0.01 mg/ml tRNA. Reactions were initiated by adding a solution containing RNA substrate (0.75, 1, 1.5, 2, 5, or 25 nM) and inhibitor (0, 3, 9, or 15 nM) in 1×annealing buffer with 0.01 mg/ml tRNA. Reactions were incubated at room temperature and time points, quenched in five volumes of formamide buffer with 80 mM EDTA, were taken every 2 min out to 40 min. Up to the first 10% of the reaction was used to find the initial velocities. Inverse substrate concentration versus inverse initial velocities were plotted on a Lineweaver–Burk plot and the K_M and V_{max} were determined using the equation [41]: $1/v = 1/V_{max} + K_M/V_{max}*1/[S]$.

Alkaline hydrolysis

1 nM of 5′ end-labeled substrate was incubated in 50 mM sodium bicarbonate, pH 9.3 at 90°C for 0, 1, 5, 15, 30, 60, and 180 min. Samples were run on a 20% acrylamide/1×TBE/7 M urea gel. Hydrolytic cleavage was quantified on a PhosphorImager (MD).

Nuclease cleavage

1 nM of 5′ end-labeled oligonucleotides were incubated with 0.1 mg/ml RNase A in 50 mM HEPES, pH 7.0, and 1 mM EDTA, 2 μg/ml nuclease P1 in 15 mM sodium acetate, pH 5.3, and 1 mM ZnCl$_2$, 10 U nuclease S7 in 100 mM sodium borate, pH 8.6, and 1 mM CaCl$_2$, or 4 U nuclease S1 in 0.6 M sodium acetate, pH 4.6, 0.1 M NaCl, and 2 mM zinc acetate at 37°C. Aliquots were removed at time points between 30 s and 2.5 h, samples run on a a 20% acrylamide/1×TBE/7 M urea gel, and fraction cleaved quantified on a PhosphorImager (MD).

Acknowledgements

References

1. Michel, F. & Westhof, E. (1990). Modelling of the three-dimensional architecture of group I catalytic introns based on comparative sequence analysis. *J. Mol. Biol.* **216**, 585–610.
2. Damberger, S.H. & Gutell, R.R. (1994). A comparative database of group I intron structures. *Nucleic Acids Res.* **22**, 3508–3510.
3. Cech, T.R., Zaug, A.J. & Grabowski, P.J. (1981). In vitro splicing of the ribosomal RNA precursor of *Tetrahymena:* involvement of a guanosine nucleotide in the excision of the intervening sequence. *Cell* **27**, 487–496.
4. Doudna, J.A. & Doherty, E.A. (1997). Emerging themes in RNA folding. *Fold Des.* **2**, R65–R70.
5. Cech, T.R. (1987). The chemistry of self-splicing RNA and RNA enzymes. *Science* **236**, 1532–1539.
6. Rajagopal, J., Doudna, J.A. & Szostak, J.W. (1989). Stereochemical course of catalysis by the *Tetrahymena* ribozyme. *Science* **244**, 692–694.
7. Zaug, A.J. & Cech, T.R. (1986). The intervening sequence RNA of *Tetrahymena* is an enzyme. *Science* **231**, 470–475.
8. Piccirilli, J.A., Vyle, J.S., Caruthers, M.H. & Cech, T.R. (1993). Metal ion catalysis in the *Tetrahymena* ribozyme reaction. *Nature* **361**, 85–88.
9. Weinstein, L.B., Jones, B.C., Cosstick, R. & Cech, T.R. (1997). A second catalytic metal ion in group I ribozyme. *Nature* **388**, 805–808.
10. Shan, S., Yoshida, A., Sun, S., Piccirilli, J.A. & Herschlag, D. (1999). Three metal ions at the active site of the *Tetrahymena* group I ribozyme. *Proc. Natl. Acad. Sci. USA* **96**, 12299–12304.
11. Zaug, A.J., Grosshans, C.A. & Cech, T.R. (1988). Sequence-specific endoribonuclease activity of the *Tetrahymena* ribozyme: enhanced cleavage of certain oligonucleotide substrates that form mismatched ribozyme–substrate complexes. *Biochemistry* **27**, 8924–8931.
12. Pyle, A.M. & Cech, T.R. (1991). Ribozyme recognition of RNA by tertiary interactions with specific ribose 2′-OH groups. *Nature* **350**, 628–631.
13. Herschlag, D. & Cech, T.R. (1990). DNA cleavage catalysed by the ribozyme from *Tetrahymena*. *Nature* **344**, 405–409.
14. Narlikar, G.J., Khosla, M., Usman, N. & Herschlag, D. (1997). Quantitating tertiary binding energies of 2′ OH groups on the P1 duplex of the *Tetrahymena* ribozyme: intrinsic binding energy in an RNA enzyme. *Biochemistry* **36**, 2465–2477.
15. McConnell, T.S., Cech, T.R. & Herschlag, D. (1993). Guanosine binding to the *Tetrahymena* ribozyme: thermodynamic coupling with oligonucleotide binding. *Proc. Natl. Acad. Sci. USA* **90**, 8362–8366.
16. Cate, J.H., Gooding, A.R., Podell, E., Zhou, K., Golden, B.L., Kundrot, C.E., Cech, T.R. & Doudna, J.A. (1996). Crystal structure of a group I ribozyme domain: principles of RNA packing. *Science* **273**, 1678–1685.
17. Golden, B.L., Gooding, A.R., Podell, E.R. & Cech, T.R. (1998). A preorganized active site in the crystal structure of the *Tetrahymena* ribozyme. *Science* **282**, 259–264.
18. Herschlag, D., Eckstein, F. & Cech, T.R. (1993). The importance of being ribose at the cleavage site in the *Tetrahymena* ribozyme reaction. *Biochemistry* **32**, 8312–8321.
19. Skorski, T., Perrotti, D., Nieborowska-Skorska, M., Gryaznov, S. & Calabretta, B. (1997). Antileukemia effect of c-myc N3′→P5′ phosphoramidate antisense oligonucleotides in vivo. *Proc. Natl. Acad. Sci. USA* **94**, 3966–3971.
20. Boulme, F., Freund, F., Moreau, S., Nielsen, P.E., Gryaznov, S., Toulme, J.J. & Litvak, S. (1998). Modified (PNA, 2′-O-methyl and phosphoramidate) anti-TAR antisense oligonucleotides as strong and specific inhibitors of in vitro HIV-1 reverse transcription. *Nucleic Acids Res.* **26**, 5492–5500.
21. Heidenreich, O., Gryaznov, S. & Nerenberg, M. (1997). RNase H-independent antisense activity of oligonucleotide N3′→P5′ phosphoramidates. *Nucleic Acids Res.* **25**, 776–780.
22. Wang, L., Gryaznov, S. & Nerenberg, M. (1999). Inhibition of IL-6 in mice by anti-NF-κB oligodeoxyribonucleotide N3′→oligodeoxyribonnucleotide N3′→P5′ phosphoramidates. *Inflammation* **23**, 583–590.
23. Gryaznov, S.M. & Winter, H. (1998). RNA mimetics: oligoribonucleotide N3′→P5′ phosphoramidates. *Nucleic Acids Res.* **26**, 4160–4167.
24. Mignet, N. & Gryaznov, S.M. (1998). Zwitterionic oligodeoxyribonucleotide N3′→P5′ phosphoramidates: synthesis and properties. *Nucleic Acids Res.* **26**, 431–438.
25. Chen, J.K., Schultz, R.G., Lloyd, D.H. & Gryaznov, S.M. (1995). Synthesis of oligodeoxyribonucleotide N3′→P5′ phosphoramidates. *Nucleic Acids Res.* **23**, 2661–2668.
26. Ding, D., Gryaznov, S.M. & Wilson, W.D. (1998). NMR solution structure of the N3′→P5′ phosphoramidate duplex d(CGCGAATTCGCG)$_2$ by the iterative relaxation matrix approach. *Biochemistry* **37**, 12082–12093.
27. Escude, C., Giovannangeli, C., Sun, J.S., Lloyd, D.H., Chen, J.K., Gryaznov, S.M., Garestier, T. & Helene, C. (1996). Stable triple helices formed by oligonucleotide N3′→P5′ phosphoramidates in-

hibit transcription elongation. *Proc. Natl. Acad. Sci. USA* **93**, 4365–4369.

28. Gryaznov, S., Skorski, T., Cucco, C., Nieborowska-Skorska, M., Chiu, C.Y., Lloyd, D., Chen, J.K., Koziolkiewicz, M. & Calabretta, B. (1996). Oligonucleotide N3′→P5′ phosphoramidates as antisense agents. *Nucleic Acids Res.* **24**, 1508–1514.

29. Rigl, C.T., Lloyd, D.H., Tsou, D.S., Gryaznov, S.M. & Wilson, W.D. (1997). Structural RNA mimetics: N3′→P5′ phosphoramidate DNA analogs of HIV-1 RRE and TAR RNA form A-type helices that bind specifically to Rev and Tat-related peptides. *Biochemistry* **36**, 650–659.

30. Tereshko, V., Gryaznov, S. & Egli, M. (1997). Consequences of replacing the DNA 3′-oxygen by an amino group: high-resolution crystal structure of a fully modified N3′→P5′ phosphoramidate DNA dodecamer duplex. *J. Am. Chem. Soc.* **120**, 269–283.

31. Testa, S.M., Gryaznov, S.M. & Turner, D.H. (1998). Antisense binding enhanced by tertiary interactions: binding of phosphorothioate and N3′→P5′ phosphoramidate hexanucleotides to the catalytic core of a group I ribozyme from the mammalian pathogen *Pneumocystis carinii*. *Biochemistry* **37**, 9379–9385.

32. Testa, S.M., Gryaznov, S.M. & Turner, D.H. (1999). In vitro suicide inhibition of self-splicing of a group I intron from *Pneumocystis carinii* by an N3′→P5′ phosphoramidate hexanucleotide. *Proc. Natl. Acad. Sci. USA* **96**, 2734–2739.

33. Matray, T.J. & Gryaznov, S.M. (1999). Synthesis and properties of RNA analogs-oligonucleotide N3′→P5′ phosphoramidates. *Nucleic Acids Res.* **27**, 3976–3985.

34. Cotton, F.A., Hazen Jr., E.E. & Legg, M.E. (1979). Staphylococcal nuclease: proposed mechanism of action based on structure of enzyme-thymidine 3′,5′-bisphosphate-calcium ion complex at 1.5-Å resolution. *Proc. Natl. Acad. Sci. USA* **76**, 2551–2555.

35. Volbeda, A., Lahm, A., Sakiyama, F. & Suck, D. (1991). Crystal structure of *Penicillium citrinum* P1 nuclease at 2.8 Å resolution. *EMBO J.* **10**, 1607–1618.

36. Zarrinkar, P.P. & Sullenger, B.A. (1999). Optimizing the substrate specificity of a group I intron ribozyme. *Biochemistry* **38**, 3426–3432.

37. Herschlag, D. & Cech, T.R. (1990). Catalysis of RNA cleavage by the *Tetrahymena thermophila* ribozyme. 1. Kinetic description of the reaction of an RNA substrate complementary to the active site. *Biochemistry* **29**, 10159–10171.

38. Strobel, S.A. & Cech, T.R. (1993). Tertiary interactions with the internal guide sequence mediate docking of the P1 helix into the catalytic core of the *Tetrahymena* ribozyme. *Biochemistry* **32**, 13593–13604.

39. Engelhardt, M.A., Doherty, E.A., Knitt, D.S., Doudna, J.A. & Herschlag, D. (2000). The P5abc peripheral element facilitates preorganization of the *Tetrahymena* group I ribozyme for catalysis. *Biochemistry* **39**, 2639–2651.

40. Narlikar, G.J. & Herschlag, D. (1996). Isolation of a local tertiary folding transition in the context of a globally folded RNA. *Nat. Struct. Biol.* **3**, 701–710.

41. Fersht, A. (1985). Enzyme Structure and Mechanism. 2nd edn., W.H. Freeman and Company, New York.

42. Shriver, D.F., Atkins, P. & Langford, C.H. (1994). Inorganic Chemistry. 2nd edn., W.H. Freeman and Company, New York.

43. McSwiggen, J.A. & Cech, T.R. (1989). Stereochemistry of RNA cleavage by the *Tetrahymena* ribozyme and evidence that the chemical step is not rate-limiting. *Science* **244**, 679–683.

44. Kyte, J. (1995). Mechanism in Protein Chemistry. Garland Publishing, Inc., New York.

45. Sambrook, J., Fritsch, E.F. & Maniatis, T. (1989). Molecular Cloning: a Laboratory Manual. 2nd edn., Cold Spring Harbor Laboratory Press, Plainview.

46. Scaringe, S.A., Francklyn, C. & Usman, N. (1990). Chemical synthesis of biologically active oligoribonucleotides using β-cyanoethyl protected ribonucleoside phosphoramidites. *Nucleic Acids Res.* **18**, 5433–5441.

47. Zaug, A.J. & Cech, T.R. (1995). Analysis of the structure of *Tetrahymena* nuclear RNAs in vivo: telomerase RNA, the self-splicing rRNA intron, and U2 snRNA. *RNA* **1**, 363–374.

48. Fraser, M.J. & Low, R.L. (1993). Fungal and mitochondrial nucleases. In *Nucleases*. (Linn S.M., Lloyd R.S. & Roberts, R.J., eds.), 2nd edn., pp. 171–207, Cold Spring Harbor Press, Plainview.

49. Gerlt, J.A. (1993). Mechanistic principles of enzyme-catalyzed cleavage of phosphodiester bonds. In *Nucleases*. (Linn S.M., Lloyd R.S. & Roberts, R.J., eds.), 2nd edn., pp. 1–34, Cold Spring Harbor Press, Plainview.

50. Strobel, S.A. & Ortoleva-Donnelly, L. (1999). A hydrogen-bonding triad stabilizes the chemical transition state of a group I ribozyme. *Chem. Biol.* **6**, 153–165.